Investigation of factors influencing the hydrolytic degradation of single PLGA microparticles

KELES, Hakan, NAYLOR, Andrew, CLEGG, Francis <http://orcid.org/0000-0002-9566-5739> and SAMMON, Chris <http://orcid.org/0000-0003-1714-1726>

Polymer Degradation and Stability 119 (2015) 228–241

Contents lists available at ScienceDirect

Polymer Degradation and Stability

journal homepage: www.elsevier.com/locate/polydegstab

Investigation of factors influencing the hydrolytic degradation of single PLGA microparticles

Hakan Keles [a], Andrew Naylor [b], Francis Clegg [a], Chris Sammon [a, *]

[a] Sheffield Hallam University, Materials and Engineering Research Institute, Sheffield, S1 1WB, UK
[b] Critical Pharmaceuticals Limited, BioCity, Pennyfoot Street, Nottingham, NG1 1GF, UK

ARTICLE INFO

Article history:
Received 11 March 2015
Received in revised form
15 April 2015
Accepted 27 April 2015
Available online 12 May 2015

Keywords:
Polymer degradation
PLGA
Controlled release
ATR-FTIR spectroscopic imaging
Gamma-irradiation
Degradation rate

ABSTRACT

Poly lactide-co-glycolide (PLGA) is an important polymer matrix used to provide sustained release across a range of active pharmaceutical ingredients (APIs) and works by hydrolytic degradation within the body, thereby releasing entrapped drug. Processing and sterilisation can impact on the morphology and chemistry of PLGA therefore influencing the hydrolysis rate and in turn the release rate of any entrapped API. This paper has looked at the effect of supercritical carbon dioxide ($scCO_2$) processing, gamma irradiation, comonomer ratio and temperature on the hydrolysis of individual PLGA microparticles, using a combination of Attenuated Total Reflectance-Fourier Transform Infrared (ATR-FTIR) imaging, Scanning Electron Microscopy (SEM), Differential Scanning Calorimetery (DSC) and Gel Permeation chromatography (GPC) to facilitate a better understanding of the physiochemical factors affecting the hydrolysis rate. This work has shown that $scCO_2$ processing influences hydrolysis rates by increasing the porosity of the PLGA microparticles, increasing the lactide comonomer ratio decreases hydrolysis rates by reducing the hydrophilicity of the PLGA microparticles and increasing the gamma irradiation dose systematically increases the rate of hydrolysis due to reducing the overall molecular weight of the polymer matrix via a chain scission mechanism. Moreover this work shows that ATR-FTIR imaging facilitates the determination of a range of physicochemical parameters during the hydrolysis of a single PLGA microparticle including water ingress, water/polymer interface dimensions, degradation product distribution and hydrolysis rates for both lactide and glycolide copolymer units from the same experiment.

1. Introduction

As a result of recent research in molecular and cell biology to meet clinical needs, the interest in biologics (a variety of therapeutics such as vaccines, recombinant proteins and peptides, genes, viruses and synthetic tissues) has intensified leading to a strong market growth, consequently currently hundreds of recombinant proteins and peptides are in the pipeline for U.S. Food and Drug Administration (FDA) approval [1]. In particular controlled release protein formulations in the form of microparticles, which release protein upon degradation of the carrier matrix, are being developed at a rapid rate as they change the period between injections from a few days to several weeks, enhance the protein therapeutic effect, and therefore noticeably increase patient compliance [2–4].

Although there are numerous candidate biodegradable polymers for carrying and releasing biologics in a controlled manner in the form of microparticles, there are few that are FDA approved due to their limited biocompatibility within the human body [5,6]. Poly (lactide-*co*-glycolide) (PLGA), a random copolymer of poly(glycolic acid) (PGA) and poly(lactic acid) (PLA), is an FDA approved biodegradable synthetic polyester that is physically stable and highly processable [6–9]. Hence, PLGA, in the form of microparticles, has been the most studied carrier matrix for macromolecules such as proteins, DNA, RNA, vaccines and peptides for treatment of several important diseases including cancer [10–13]. Another advantage of PLGA is that its degradation *in vivo*, which governs the drug release, is controllable mainly by choice of comonomer ratio (i.e. lactide to glycolide (*L/G*)), microparticle morphology and to a lesser extent molecular weight; it also yields lactic and glycolic acids, which are biocompatible and rapidly cleared from the body via the renal system [5].

In order to produce microparticles that release drugs effectively, the drug needs to be mixed with in the polymer(s) homogenously and this is highly dependent on liquefication of the polymer(s)

* Corresponding author. Tel.: +44 (0)114 225 3069; fax: +44 (0)114 225 3501.
E-mail address: C.Sammon@shu.ac.uk (C. Sammon).

http://dx.doi.org/10.1016/j.polymdegradstab.2015.04.025

during the formation of particles. Common methods for producing sustained release drug delivery systems, which differ mainly in how they are liquefied include; spray drying [14], emulsification processes (single and double) [13] and more recently using a supercritical fluid-based Particles from Gas Saturated Solution (PGSS) process in a novel way, i.e. CriticalMix™. Unlike the aforementioned methods, CriticalMix™ has the advantage in that it works in the absence of organic solvents and the polymer and drugs do not need to be soluble in $scCO_2$. However the polymer does need to be sufficiently plasticised by $scCO_2$, which can be achieved at moderate temperatures (typically <40 °C) and pressures (<150 bar) that have no adverse effect on protein stability within controlled release PLGA/PLA formulations [15].

It is well known that polymer morphology has a role in the degradation of microparticles and that $scCO_2$ creates porosity, therefore the first aim of this work was to characterise the physiochemical effects of $scCO_2$ processes on the *in vivo* degradation of a PLGA 50/50 microparticle using ATR-FTIR imaging for the first time.

Understanding polymer degradation is critically important for modifying the performance of any biodegradable polymeric drug delivery system. PLGA degrades via chain scissions of ester bond linkages in the polymer backbone by hydrolytic attack of water molecules [16,17]. Factors effecting the hydrolytic degradation of PLGA devices in the form of microspheres [18,19], porous scaffolds [20], dense films [21] and cylinders [22,23] have been widely studied. In recent work by the authors it has been shown that FTIR imaging in ATR mode using a focal plane array detector coupled with multivariate analysis has provided visual evidence of morphological and physiochemical changes during hydrolysis of a PLGA microparticle *in situ*. Quantitative information including hydrated layer size surrounding the particle, width of the particle and perhaps more importantly the degradation rate of individual glycolic and lactic units in real time, the latter of which was reported to be calculated more accurately using the novel non-linear curve fitting procedure compared to traditional peak height image analysis [24]. Using the same experimental procedure and relevant image analysis methods developed by the authors the degradation characteristics of a family of PLGA microparticles with L/G molar compositions of 100/0, 75/25 and 50/50 in water are reported herein by calculating the hydrolytic degradation rate of the individual lactic and glycolic acid units and relating to morphological changes.

Biodegradation of a PLGA microparticle studied by the authors using FTIR imaging in ATR mode was observed to occur through a hydrolytic chain cleavage mechanism and the rates of polymer degradation were similar for both the surface and bulk microparticles [24]. Since degradation of the PLGA microparticles generates acidic monomers, μpH distribution mainly within the bulk has been one of the important questions concerning protein stability within degrading PLGA microparticles. Several groups have quantified μpH in PLGA matrices by several methods including; nuclear magnetic resonance (NMR) [25], electron paramagnetic resonance (EPR) [26], and confocal fluorescence microscopy using various dyes as labels [27–29]. Although reported results on pH distribution in degrading polymers vary, it is well established that the acidic monomer distribution mainly depends on the morphology and shape of the microparticle which is, in turn, mainly governed by the production method [27]. Herein a single PLA microparticle has been evaluated within a 640 μm × 640 μm field of view using FTIR imaging in the ATR mode and the inherently rich chemical signal of mid-IR vibrations without any chemical label or dye for the first time.

Jordan et al. [30] showed that novel sustained release PLGA/PLA microparticles formulations containing human growth hormone (hGH) could be prepared by the CriticalMix™ process with 100% encapsulation efficiency. This formulation has been shown to demonstrate >2 weeks longer efficacious hGH release compared to a daily injection of soluble hGH *in vivo* in rats and monkeys and *in vitro* [3]. This same formulation has been investigated for its real time release using ATR-FTIR imaging for the first time [31]. The study also evaluated the effect of γ-irradiation, a well-established method to sterilise polymeric microparticle drug delivery systems before use, on their physical and chemical structure. The release mechanism of hGH was elucidated with respect to the release kinetics changing as a result of modifications to the microparticle morphology and chemistry during γ-irradiation. This finding raised important questions regarding their degradation. Interestingly, spectroscopic changes resulting from γ-irradiation on bulk PLGA 50/50 were not detected using FTIR spectroscopy, however the observation that protein release from a PLGA 50/50 microparticle was noticeably different to that of a γ-irradiated microparticle, encouraged us to determine if the un-irradiated and γ-irradiated PLGA 50/50 microparticles in the absence of hGH would degrade differently due to morphological changes. Therefore the final aim was to answer this question and help form fundamental links between the release characteristics of an important controlled release matrix and hydrolysis rates.

2. Experimental

2.1. Materials

PLGA RG502H (50:50 lactide:glycolide, I.V. 0.16–0.24, Bohringer-Ingleheim), PLGA RG752H (75:25 lactide:glycolide, I.V. 0.16–0.24, Bohringer-Ingleheim) PLA R202H (100:0 lactide:glycolide, I.V. 0.16–0.24, Bohringer-Ingleheim), pharmaceutical grade CO_2 (BOC Special Gasses) were used as received. Lactic acid (DL-Lactic acid, W261114, Sigma-Aldrich Company Ltd.) was dried at 70 °C for 1 day before use. Water used in the experiments was purified using a ELGA Purelab option-R water distiller (Up to 15 MΩ-cm, Type II water) and degassed using a Fisherbrand FB11004 ultrasonic bath at the relevant temperature (50 °C or 70 °C) for 15 min.

2.2. CriticalMix™ processing of PLGAs

CriticalMix™ is a novel one-step PGSS process used to produce microparticles with 100% encapsulation efficiency [30,32]. The method of PGSS, uses the ability of $scCO_2$ to depress the glass transition or melting temperature of polymers at ambient temperatures and moderate pressures. $scCO_2$ acts effectively as a molecular lubricant, thus liquefying polymers at temperatures significantly lower than those typically needed. This liquefication of the polymers allows APIs such as peptides and proteins that remain in the dry state during processing to be easily dispersed within the polymer matrix. CO_2 is the ideal choice for this application as it is readily available, non-toxic and interacts strongly with many biodegradable amorphous polyesters. In addition, the process is not drug specific and could provide a route to manufacturing many sustained release drug products across the pharmaceutical industry. The near ambient temperatures together with the absence of any aqueous or organic solvents makes the PGSS method particularly suited to the processing of thermally or solvent labile proteins and peptides, with the advantage that they can be encapsulated with no degradation or loss of activity. When suitable polymers such as PLGA, poly(ethylene glycol) or poloxamer and proteins such as bovine serum albumin or human growth hormone are exposed to $scCO_2$ in a pressure vessel, the polymer is liquefied, following mixing the mixture is depressurised through a nozzle whereby the CO_2 returns to a gaseous state by evaporation and the polymer solidifies. The batches used in this study were prepared

using only PLGAs by adding 2.1 g of pre-weighed polymer, to the PGSS apparatus which was then sealed, pressurised with CO_2 to 700 psi (48 bar) and heated to 40 °C. Once at temperature, the pressure was increased to 2030 psi (140 bar). The liquefied polymer was then stirred at 150 rpm for 1 h, after which time stirring was stopped and the mixture was depressurised through a nozzle into a cyclone and recovered as free flowing white powder.

2.3. γ-Irradiation

10 mg of unprocessed PLGA50/50 polymer was sealed in a glass vial containing air and γ-irradiated at 25 or 100 kGy total dose by using ^{60}Co as the irradiation source (Synergy Health PLC, Swindon, UK) in accordance with the ISO 11137 standard.

2.4. Scanning electron microscopy

To investigate the morphology of the PLGA microparticles, SEM was performed using a FEI NOVA 200 NanoSEM and images were formed using the secondary electron signal with a spatial resolution of ~2 nm. All samples were sputter coated at the same time with gold (~20 nm) in an Argon atmosphere to enhance secondary electron emission and reduce charging.

2.5. Molecular weight determination of the γ-irradiated and control PLGA 50/50s

Gel permeation chromatography (GPC) was performed on a PL-120 (Polymer Labs) with a differential refractive detector used to analyse the molecular weight of the control and γ-irradiated PLGA 50/50 samples. After drying, THF (1.2 ml) was added to each Eppendorf tube containing the samples and placed on a vibrating plate for 1 h to aid dissolution. Once dissolved, the mixture was filtered through a 0.2 μm filter. For GPC analysis two 30 cm Polargel Mixed-C columns in series were eluted by THF and calibrated with narrow poly(styrene) standards. The calibration and analyses were performed at 40 °C with a THF flow rate of 1 ml/min. The GPC data was analysed using Cirrus software (version 2.0, Polymer Laboratories).

2.6. Differential scanning calorimetry (DSC)

DSC was used to determine the glass transition temperature (T_g) on a range of un-irradiated, un-processed and γ-irradiated PLGA50/50 samples. Measurements were conducted by sealing 2 mg of sample within an aluminium Tzero pan. Data was collected using a TA Instruments Q2000 DSC, calibrated with an Indium standard, under N_2 with a heating rate of 10 °C/min.

2.7. Macro ATR-FTIR imaging of reactions with the Golden Gate™ sampling accessory

Hydrolysis experiments were conducted using an Agilent 680-IR FT-IR spectrometer attached to a large sample external compartment holding a Golden Gate™ Imaging Single Reflection ATR Accessory (Specac Ltd.) which has a diamond internal reflection element providing imaging with a 640 μm × 640 μm field of view and ~18 μm spatial resolution that is coupled to a liquid nitrogen cooled MCT-FPA detector. Individual microparticles (<200 μm) were selected and placed on to the ATR crystal (640 μm × 640 μm) with a needle (Agar Scientific microtool straight needle T5340) using a 40× binocular microscope and raw image data was collected using the Agilent Technologies' ResolutionsPro FTIR Spectroscopy software version 5.2.0 (CD846) within the mid-infrared (3800–950 cm^{-1}) region with 4 cm^{-1} spectral resolution under the conditions described elsewhere [24] at 50 °C or 70 °C where indicated.

2.8. Analysis of Mid-IR images

Spectra that make up the raw FTIR images were cropped between 1820 and 1000 cm^{-1} which include at least 11 characteristic bands associated with PLGA and also the water δ(OH) peak at ~1635 cm^{-1}. The cropped data was first order baseline corrected and vector normalised. 'Water' and 'PLGA' images were then generated using software MCRv1.6 as described in Ref. [24]. The data used to generate line profiles to investigate polymer–water interfaces and to calculate the degradation rate constants were processed using the non-linear curve fitting algorithm developed by authors as described elsewhere [24]. As the error obtained when calculating rate constants by binning a number of spectra (5 × 5 pixels) was found to be lower than that obtained from a single pixel, three 5 × 5 pixel regions of interest were selected from each experiment for each sample. Binned spectra of these regions were used to calculate rate constants [24].

3. Results and discussion

3.1. The effect of $scCO_2$ process on morphology and hydrolytic degradation of PLGA microparticles

It is a well-known finding that $scCO_2$ processed polymer microparticles possess a porous morphology mainly because the escaping CO_2 form bubbles that push against the solidifying polymer [32–34]. Porosity is a key advantage in producing micron sized drug delivery devices because it enhances the diffusion based release of the drug molecules as a result of increased surface area [31]. However the CO_2 pressure must be controlled well in order to avoid macroporosity and for the CriticalMix™ process, the porosity and particle size were shown to be controllable parameters; by changing the temperature or pressure of the $scCO_2$ in the mixing vessel, the viscosity of the liquefied mixture was shown to change significantly, allowing further control of particle size and morphology [33].

The effect of $scCO_2$ processing on the microparticle morphology was investigated using SEM which is a well-established imaging modality used in the microscopic characterisation of particles and other polymer surfaces [35]. Fig. 1A shows SEM images, obtained under the same conditions from two particles of un-processed PLGA 50/50 polymers. SEM images of two microparticles from the same polymer which have undergone CriticalMix™ processing are shown in Fig. 1B. As one can immediately observe, in Fig. 1B the processed particles have numerous pores ~1–5 μm diameter and in comparison, the un-processed microparticles in Fig. 1A have a rougher surface topography with fewer pores, that would likely inhibit the ingress of solvent (water in the case considered here) when subjected to it. Comparing Fig. 1A and B; it can be seen that the $scCO_2$ process does create porosity, however no macroporosity could be observed which indicates the success of the CriticalMix™ process.

In order to facilitate an insight to the effect of the $scCO_2$ processing (which resulted in a porous structure) on the hydrolytic degradation behaviour of the PLGA 50/50 polymer, FTIR imaging in ATR mode was used as demonstrated in previous work [24]. For the real-time hydrolytic degradation, two PLGA 50/50 microparticles; un-processed and CriticalMix™ processed, were placed on to the ATR crystal at 70 °C and their interaction with water at 70 °C was monitored.

Fig. 2A and B shows the temporal distribution as MCR-ALS deconvoluted IR images for PLGA 50/50 in the top row and water

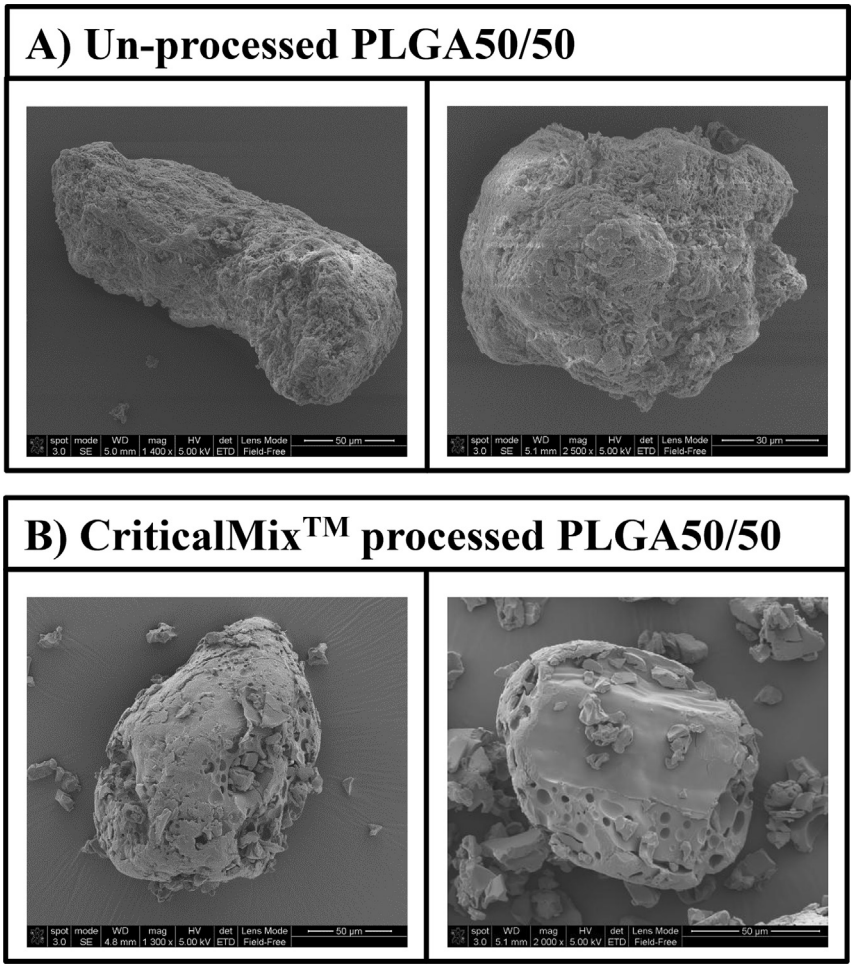

Fig. 1. A set of SEM images of 2 particles in each row showing un-processed (A) and CriticalMix™ processed (B) PLGA 50/50 microparticles.

in the bottom row, for an un-processed and a CriticalMix™ processed microparticle, respectively. The 0 h images in both Fig. 2A and B were collected over a period of ~5 m immediately after the water was added into the system. Even within this short collection time, there is evidence of an interface layer of hydrated PLGA surrounding both the processed and un-processed particles, as indicated by the apparent concentration gradient from the particle centre towards the water rich zone. It is also evident that some water ingresses immediately into the whole field of view within the 5 min period, possibly between the particle and ATR crystal regardless of porosity since the calculated water concentration is not quite zero. However although the water concentration is quite low in the 0 m images of both particles as indicated by the blue colour in the centre (or core), at the following time points, there is much more water with in the centre of the processed microparticle (turning from light blue to green as time proceeds) in comparison to the un-processed particle (a dark blue area that decreases in size as time proceeds). The PLGA images that anticorrelate with the water images in both Fig. 2A and B shows a decrease in the size of the core region (red zone in the 0 h images) with increasing time points. However when one compares the last 3 PLGA images of un-processed and processed microparticles, it can be seen that the core of the processed particle almost completely disappears turning to yellow and light blue in 6.5 h and 8 h images, respectively, whereas a red zone at the centre of the un-processed microparticle still exists even after 9 h of water contact.

When water is introduced into the system, there are 3 domains; only water, regions in which polymer is the dominant signal and others in which a mixture of water and polymer were observed; a hydrated polymer zone. To facilitate better comparison between the different microparticle systems, two parameters were extracted from each polymer response profile) as shown in previous studies [24]), namely the full width at half maximum height (FWHM) of the polymer core size and the size of the hydrated polymer layer to the right hand side of the profile where the polymer intensity is <90% of its maximum value and >10% of its minimum value (B). The parameters B and FWHM were generated using the non-linear curve fitted (NLCF) spectra for 3 consecutive parallel lines (of which the standard deviation between these 3 lines was used to generate the error bar) along the core of the microparticles as it provided slightly better spatial resolution in comparison to MCR-ALS images., This approach was not used for generating the full image sets shown in Fig. 2, due to the time penalty, NLCF processing of 3 lines of 64 pixels was deemed to be affordable as discussed in detail in Ref. [24].

Fig. 3A shows the evolution of the right hand side hydrated zone (B) and FWHM of the unprocessed microparticle. Although an increase in the hydrated zone is observed overtime, the FWHM of the particle appeared to be quite steady; not showing much swelling or decrease in size, indicating little water ingress in to this zone as discussed previously. Fig. 2B shows the analogous plots of B and FWHM this time for the CriticalMix™ processed microparticle. The change in size of the right hand side hydrated layer or B seems to be very similar to that of the un-processed particle in Fig. 3A. This

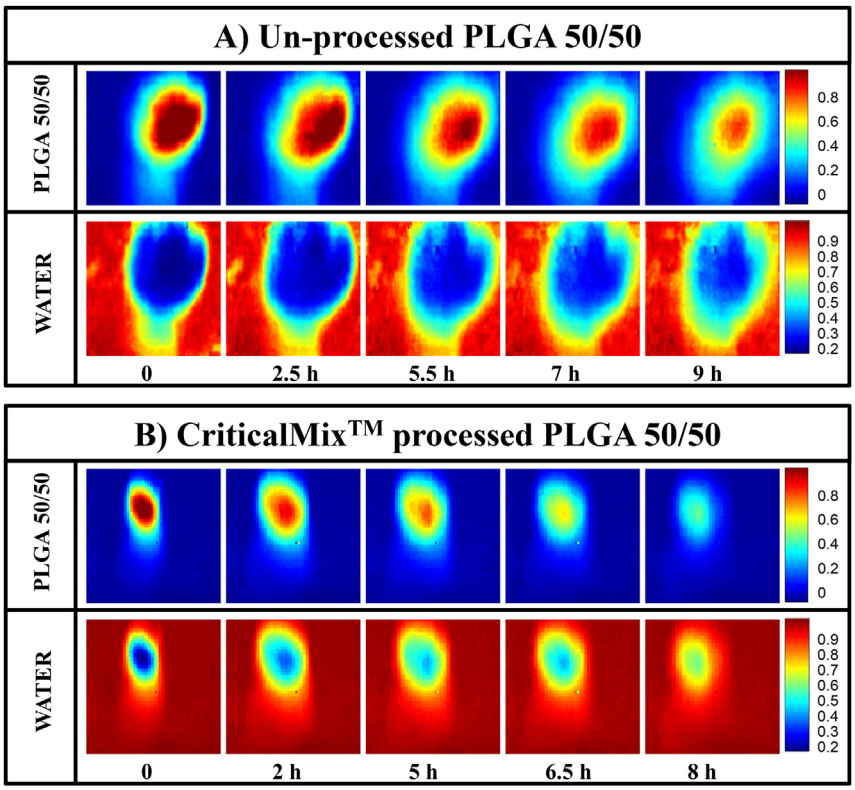

Fig. 2. (A) Jet colour FTIR images representing temporal distribution of un-processed PLGA50/50 on the top and water at the bottom and (B) analogous images obtained from a $scCO_2$ processed microparticle. (For interpretation of the references to colour in this figure legend, the reader is referred to the web version of this article.)

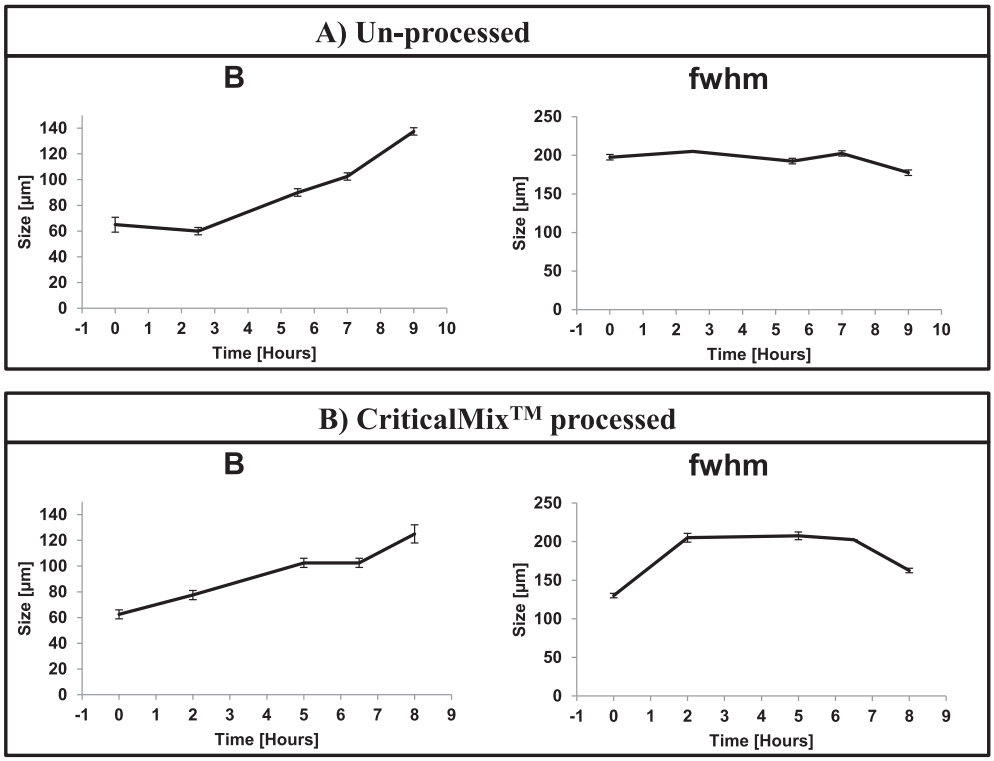

Fig. 3. The evolution of the parameter 'B', as a function of time on the left and the evolution of parameter 'A', FWHM, as a function of time on the right hand side for the un-processed (A) and CriticalMix™ processed (B) PLGA 50/50.

could indicate that the magnitude of the hydrated zone was independent on porosity however, it should also be noted that this argument is only valid within a regime with a spatial resolution of ~43 μm and if there was any difference less than this it would be difficult to probe or compare. The FWHM of the processed microparticle is quite different to that of the unprocessed microparticle, in that the former after an initial swelling decreases to a much greater extent in comparison. This was thought to be an indication of more water accessing the core of the particle through the pores, causing faster degradation and hence the greater decrease in its FWHM compared to that of un-processed microparticle.

As demonstrated previously [24] deconvolution using NLCF permits the use of the relative intensities of two infrared bands at ~1452 cm^{-1} and ~1424 cm^{-1} (corresponding to the antisymmetric bending of CH_3 from the lactic acid units and the symmetric bending of CH_2 from the glycolic acid units) to determine the rate of hydrolysis of the two co-polymer segments within the same experiment. Using the same procedure for three 5 × 5 binned pixels of selected regions within the temporal image sets the degradation rate constants were calculated for both processed and unprocessed PLGA 50/50. Calculated rate constants for lactic and glycolic units for the two polymers at 70 °C are listed in Table 1. Unprocessed PLGA 50/50 was found to degrade slower than processed PLGA 50/50, which is expected as the latter are more porous. This result was in agreement with those obtained by Odelius et al. [20] who studied hydrolytic degradation of polylactide (PLA) scaffolds with porosities above 90% and different pore size ranges. They showed that both porosity and pore size regulated the degradation rate of porous PLA scaffolds and that the degradation rate of the porous structures decreased with decreasing pore size.

Interestingly for both microparticles, glycolic units were found to degrade ~1.3 times faster than lactic units. It was also interesting that although polymer morphology was shown to have an impact on degradation rate and swelling behaviour as discussed previously, the lactic and glycolic units were found to degrade at an almost constant rate with respect to each other independently of morphology. This agrees with the findings reported by Vey et al. that glycolic units were found to degrade ~1.3 times faster than the lactic units in a range of PLGA films [21] in phosphate buffer solution.

3.2. The effect of composition and temperature on hydrolytic degradation kinetics of $scCO_2$ processed PLGA

As a kinetic process temperature will impact upon hydrolysis rate, it has also been frequently reported that copolymer ratio (i.e. LA:GA) is a significant factor governing the hydrolytic degradation rate of PLGA [16,19,21,36,37]. In order to understand the tuning criteria for the degradation of $scCO_2$ processed PLGA microparticles, a range of compositions of CriticalMix™ processed PLGA (Table 2) were studied in the presence of water at 70 °C and 50 °C.

Fig. 4A–C shows five false colour MCR-ALS images of the $scCO_2$ processed PLGA 100/0 (or PLA), PLGA 75/25 and PLGA 50/50 microparticles, respectively undergoing hydrolysis at 70 °C. The polymer distribution is given at the top and the water distribution is given at the bottom, at different time points for each composition of PLGA. Comparing the polymer distribution images for each composition at 70 °C in A, B and C, it can be seen that the polymer core (indicated by the darkest red colour in the upper image set) decreases in all three PLGA image sets as a function of time, however this decrease can be seen to occur at a higher rate as the LA:GA ratio decreases. Although PLA exhibits an ongoing swelling behaviour (yellow, green and light blue regions) with a slightly decreasing polymer core zone (red) even at the 24 h time point, PLGA 75/25 and PLGA 50/50 have almost completely hydrolysed within ~5 h, with almost no core area (red) remaining. Instead one can observe a highly hydrated polymer rich region (yellow) clearly at 9 h in PLGA 75/25 and even earlier in PLGA 50/50 at 6.5 h. The corresponding water images show a strong anti-correlation with the polymer particle images and the colour and by inference the water content within the microparticles follows that expected when LA:GA ratio is changed, i.e. increasing the GA content increases the hydrophilicity of the polymer, leading to an increase in rate of the water content and an increase in the hydrolysis rate.

Table 1
List of calculated degradation rates in day^{-1} for glycolic and lactic units and their ratios for unprocessed and processed PLGA50/50.

PLGA 50/50	kL	kG	kG/kL
Un-processed	0.98 ± 0.12	1.26 ± 0.14	1.28
CriticalMix™ Processed	1.71 ± 0.21	2.27 ± 0.24	1.32

Table 2
List of PLGA samples studied where *L/G* is the copolymer lactic/glycolic units molar ratio, M_n is the number average molecular weight, M_w is the weight average molecular weight, PDI is the polydispersity (M_w/M_n) and T_g is the glass transition temperature.

PLGA	L/G	M_n (g/mol)	M_w (g/mol)	PDI	T_g (°C)
RG502H	50/50	131	5075	38.74	45.7
RG752H	75/25	3063	8722	2.84	47
RG202H	100/0	5758	12,170	2.11	51

Fig. 5A–C show the FWHM and the hydrated layer size at 70 °C as a function of degradation time for PLA, PLGA 75/25 and PLGA 50/50, respectively. In Fig. 4A after an initial swelling, the FWHM of the PLA microparticle becomes almost constant, as one would expect at an early stage of hydrolytic degradation. Both FWHMs of the PLGA 75/25 and PLGA 50/50 microparticles in Fig. 5B and C, respectively indicate an initial swelling which is slightly more apparent for PLGA 50/50. After ~7 h the FWHM of the PLGA 50/50 decreases (Fig. 5C) whereas the FWHM of the PLGA 75/25 increases (Fig. 5B). This may well be the result of the images showing different degradation stages; in Fig. 4B. PLGA 75/25 can be seen to almost disappear at 9 h whilst in comparison, in Fig. 4C, PLGA 50/50 still has a core that is decreasing in size. Comparing the water distribution images of PLGA 75/25 (Fig. 4B) and PLGA 50/50 (Fig. 4C) it can be determined that there is more water in the core of PLGA 75/25 microparticle at 7 and 9 h than that of PLGA 50/50 microparticle. This could be explained by examining the morphology of the microparticles. Fig. 6A–C show two SEM images each for PLGA 50/50, PLGA 75/25 and PLA microparticles, respectively. Although the morphology of the PLGA 50/50, PLGA 75/25 and PLA look broadly similar the pore size of the PLGA 75/25 particles in Fig. 6B are somewhat larger than those of PLGA 50/50 microparticles shown in Fig. 6A. Therefore it should be anticipated that water would diffuse into the PLGA 75/25 microparticle at a greater extent than into the PLGA 50/50 microparticle, due to the PLGA 50/50 microparticle having narrower pathways.

An interface layer of hydrated PLGA around the particle starting from the 0 h PLGA images in Fig. 4A–C can be seen quite clearly for all three microparticles. However, although the thickness of this hydrated layer (light blue to yellow) is roughly similar sized within the first two images of the polymers in comparison to each other, in the last three images the hydrated layer of PLGA 75/25 and PLGA 50/50 are broader than those of the PLA. This observation was also quantified by plotting the parameter B that represents the hydrated layer size. Comparing the hydrated layer size of PLA over time in Fig. 5A to that of PLGA 75/25 in Fig. 5B and PLGA 50/50 in Fig. 5C, it can be seen that although hydrated layer of PLGA 75/25 and PLGA 50/50 increases from ~60 to ~100 μm within 5 h, the hydrated layer

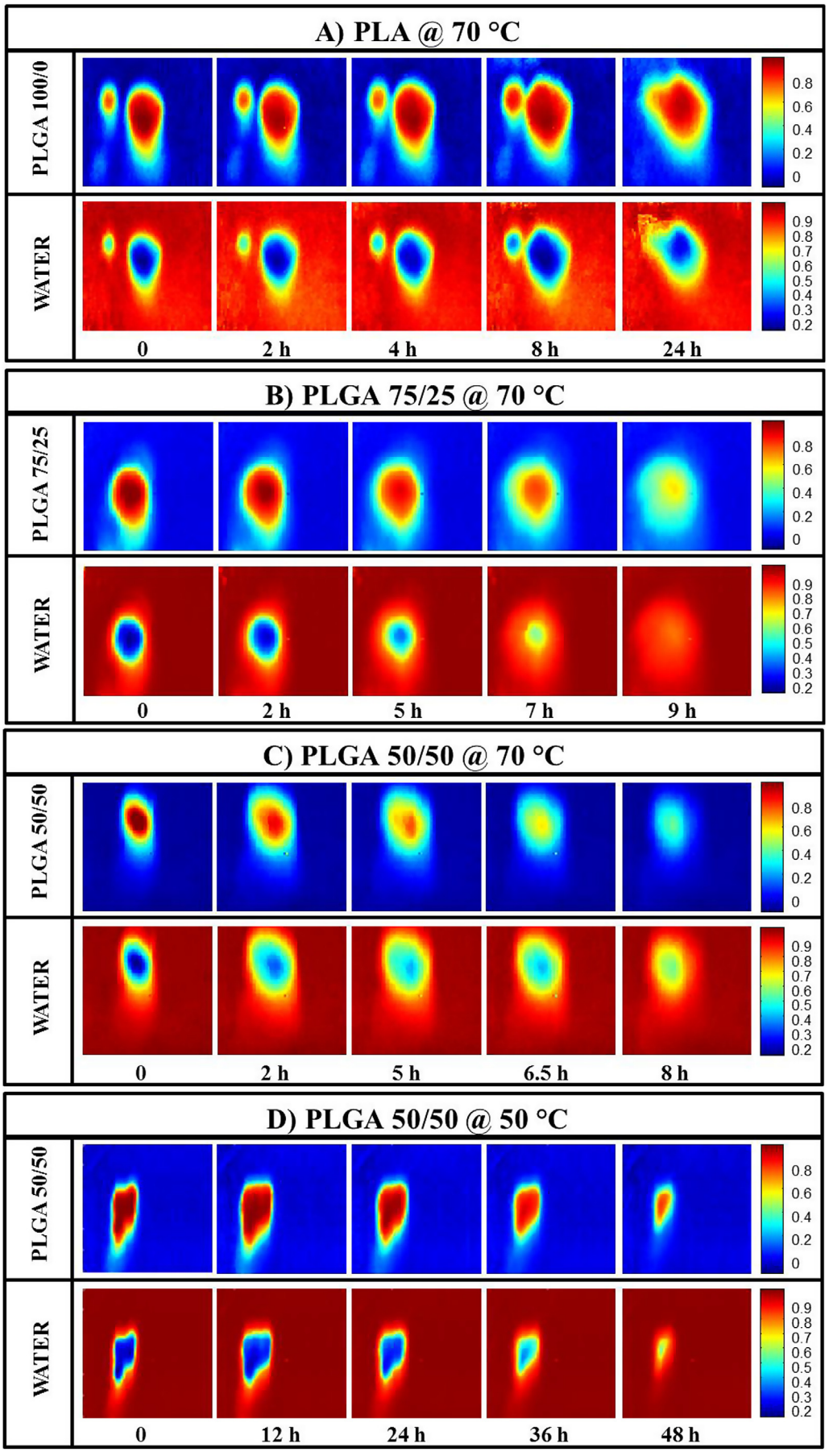

Fig. 4. Jet colour MCR-ALS processed images representing temporal distribution of PLGA at the top and water at the bottom for $scCO_2$ processed PLA at 70 °C (A), PLGA 75/25 at 70 °C (B), PLGA 50/50 at 70 °C (C) and PLGA 50/50 at 50 °C (D). (For interpretation of the references to colour in this figure legend, the reader is referred to the web version of this article.)

size of PLA only increases from ~50 to ~60 μm. This was thought to be a result of different hydrolysis rates being observed within the images. It could be expected that even at 24 h PLA is still at an early stage of hydrolysis, still showing early stage swelling and a consistent core size or FWHM (Fig. 5A).

Fig. 4D shows analogous images to those in Fig. 2B, of a $scCO_2$ processed PLGA 50/50 microparticle undergoing hydrolysis at 50 °C with a different time axis. An immediate difference that can be observed between the PLGA 50/50 images at 50 °C and 70 °C is that the size of the hydrated layer is much smaller at 50 °C than at 70 °C. This observation is more evident in the hydrated layer size plot in Fig. 5D as it is ~20 μm over the first 24 h with only a modest increase of ~5 μm within that time period. Even after 48 h, the hydrated layer size is only ~50 μm at 50 °C where as that of the microparticle at 70 °C increases from 60 μm to 120 μm within 8 h. An initial increase of swelling can also be observed for the PLGA 50/50 microparticle at 50 °C in the FWHM plot in Fig. 5D, which is similar to that exhibited at 70 °C (Fig. 5C) but on a shorter time scale.

The hydrolysis rates of both lactic acid and glycolic acid units of the PLGA 50/50 and PLGA 75/25 and the hydrolysis rate of PLA at both 50 °C and 70 °C were calculated and are shown in Table 3. Clearly, the glycolic acid units were once more shown to have hydrolysed ~1.3 times faster than lactic acid units, regardless of the temperature, morphology, $scCO_2$ process or composition. It is well established that increasing the glycolic acid content of PLGA polymers results in a higher hydrolysis rate, mainly because the higher hydrophilicity of glycolic repeat units results in a greater degree of water uptake during hydrolysis [19,21,37]. All 3 PLGA compositions showed a higher degradation rate for both lactic and glycolic units at 70 °C when compared with those calculated at 50 °C as expect and this finding was found to be in agreement with those of Agrawal et al. [22] who studied the elevated temperature degradation of PLGA 50/50 using GPC.

Calculation of degradation rates at 37 °C of different compositions of PLGA microspheres and mm sized discs were conducted by Tracy et al. [19] and Vey et al. [21,38], respectively. The PLGA microparticles studied here were $scCO_2$ processed resulting in a very porous structure with a much higher surface area and were conducted at a higher temperature (50 and 70 °C) therefore the rates obtained were higher than those of Tracy et al. and Vey et al. as expected [20]. Although Vey et al. studied different shaped samples of PLGA (i.e. mm sized discs) using IR and Raman spectroscopies, their data analysis approach on IR spectroscopic data was similar to the one developed here, in that they also fitted the IR bands, but to a Voigt function, and monitored the lactic and glycolic units by using fitted peak intensities at 1452 cm^{-1} and 1422 cm^{-1}, respectively [21]. Furthermore their data revealed a two stage process for degradation and their study was conducted at 37 °C in phosphate buffer solution and under these conditions their experiments lasted up to 40 days. Therefore one could easily anticipate the observation of higher degradation rates and a single stage degradation process when compared to those of Vey et al., firstly because temperatures studied here were above the T_g and secondly the samples studied here were porous microparticles rather than mm sized discs. Nevertheless, the calculated ratios between the rate constants of glycolic and lactic units here in was ~1.3, which was in agreement with those of Vey et al. The calculated k values [24] are also in reasonable agreement with each other and with the values determined by Tracy et al. [19] and Vey et al. [21] as discussed in detail previously [24].

It is well understood that molecular weight has an influence on the degradation rate of PLGA [18], those with higher molecular weight have longer polymer chains, which require more time to degrade than shorter polymer chains. However, in the case of PLA lower molecular weight is associated with higher degrees of crystallinity [18], so the relationship between Mw and degradation rate is not quite so simple. Observations of the trends shown in Table 3 would suggest that the hydrophobicity of the LA segments is playing the largest part in the determination of the measured degradation rates between different grades of PLGA.

3.3. Visual evidence of lactic acid diffusion from a degrading PLA microparticle

The degradation of PLGA involves chain scissions of ester bond linkages in the polymer backbone by hydrolytic attack of water molecules. Lactic acid and glycolic acid, which are biocompatible and rapidly cleared from the body via the renal system, are the end products of degradation [5]. PLGA degradation can result in a build-up of acidic by-products since it is made up of acidic monomers. When labile drugs such as proteins and peptides are entrapped with in PLGA microparticles, the local pH drop inside the microparticles due to trapped lactic and/or glycolic acid has been shown to cause protein instability and hydrolysis [36,39,40]. To try and determine if FTIR imaging could be used to identify a localised build-up of degradation products during hydrolysis, the data shown in Fig. 3A was investigated in greater detail.

Fig. 7A shows two false colour peak height images obtained from the hydrolysis experiment of a PLA microparticle after 12 h. The image to the left was generated by plotting the peak height of the band at 1755 cm^{-1}, which is the position of the PLA carbonyl peak maximum as can be seen in Fig. 7D, whereas the right hand side image was generated by plotting the peak maximum at 1740 cm^{-1} which is the position of the lactic acid monomer carbonyl peak maximum, as can be seen in the FTIR spectrum of lactic acid, shown in Fig. 7C. The spectrum at a specific pixel (indicated by the arrow in each image) is shown directly below the image and in Fig. 7A these correspond to PLA and water (left and right, respectively). Fig. 7C shows the analogous results to those in Fig. 7A, but this time from the 88 h image. In this instance the spectrum observed in the core of the particle appears to be dominated by PLA and water whereas the same pixel selected previously away from the particle shows strong evidence of the lactic acid degradation product and water.

PLGA 50/50 (25 kDa) microspheres prepared by a double-emulsion technique were studied by Fu et al. [28] using confocal fluorescence microscopy and probing pH-sensitive fluorescent dyes that were entrapped within the microspheres. Their study showed the formation of a very acidic environment within the particles with a minimum of pH 1.5. Their images showed a pH gradient, with the most acidic environment at the centre of the spheres and higher pH near the edges. However, the preparation method has a major effect on the morphology, structure and chemistry of the polymeric microparticles resulting in different degradation characteristics. For example, Ding et al. [27] also studied several PLGA microspheres, prepared by oil-in-oil emulsion and double emulsion methods and labelled with fluorescent dyes, using confocal laser scanning microscopy. Their work indicated that microspheres prepared by the oil-in-oil emulsion method were less acidic than those prepared by double emulsion. The distribution of lactic acid in Fig. 6B can be seen to be somewhat different to the distribution of PLA within the microparticle, if one superimposed the two images generated from bands at 1755 cm^{-1} and 1741 cm^{-1}, the implication is that the lactic acid monomer has diffused out from the microparticle into the surrounding aqueous media, since there is much less lactic acid with in the core of the PLA microparticle. This is an important finding; firstly because this is the first image showing lactic acid distribution within a degrading PLA microparticle in its natural environment (i.e. without modifying the sample

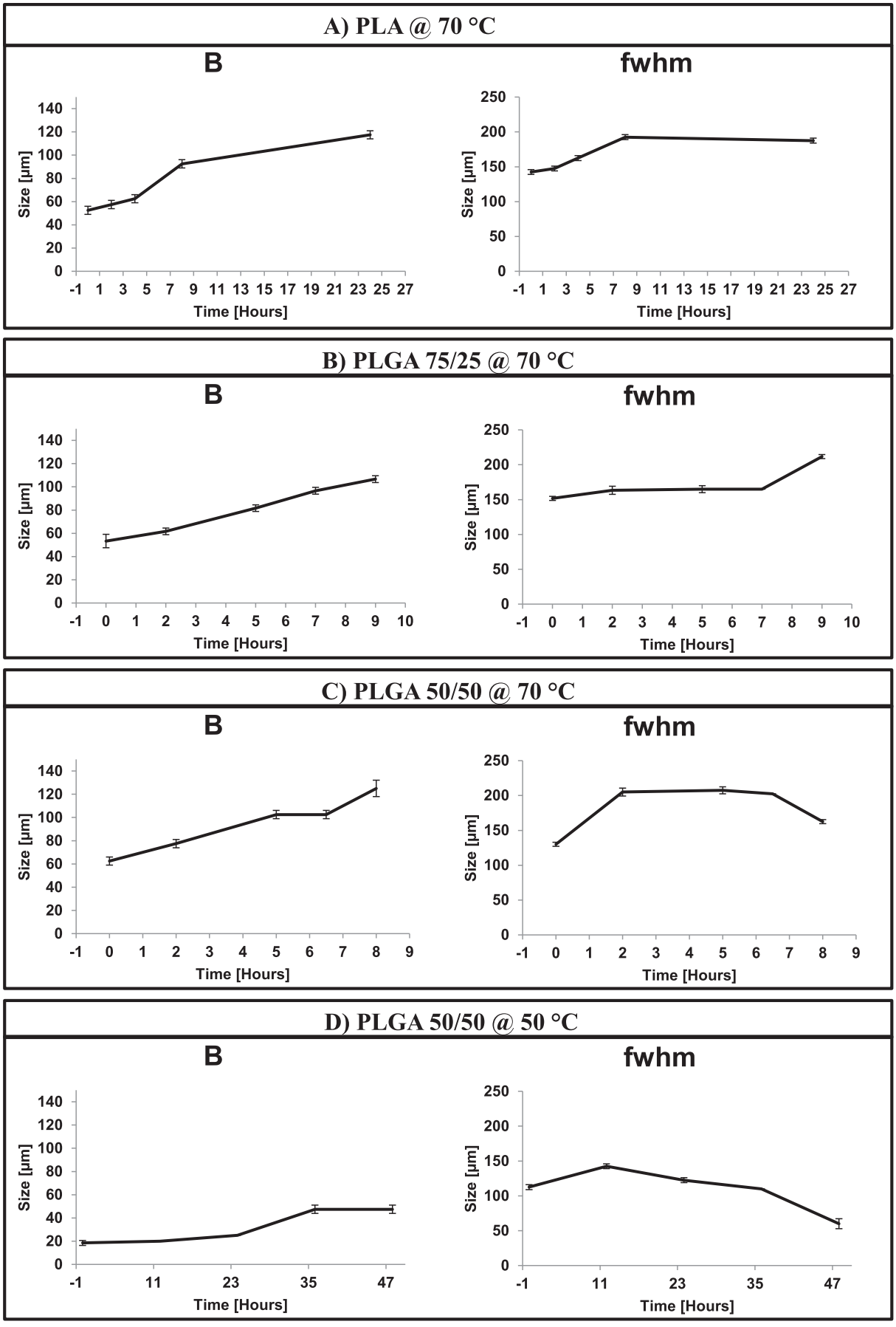

Fig. 5. The evolution of the hydrated zone, 'B', as a function of time on the left and the evolution of parameter 'A', FWHM, as a function of time on the right hand side for the $scCO_2$ processed PLA at 70 °C (A), PLGA 75/25 at 70 °C (B), PLGA 50/50 at 70 °C (C) and PLGA 50/50 at 50 °C (D).

using any chemical dyes) and secondly, there is evidence that the lactic acid molecules had diffused out of the particle during hydrolysis which would change the local environment for any labile drug molecule entrapped within or surrounding the polymer matrix.

3.4. The effect of γ-irradiation on hydrolytic degradation of PLGA 50/50

Biodegradable polymeric pharmaceuticals often have to be sterilised after manufacture and γ-irradiation is a well-established and commonly applied method for sterilising polymeric microparticle drug delivery systems [41]. Since each polymer may respond differently to ionizing radiation, it is essential to determine any effects that the sterilisation process may have on the drug carrier, in this case PLGA. Therefore the effect of a range of γ-irradiation doses on PLGA 50/50, which made up 90 wt% of the CriticalMix™ produced formulation studied in bulk [30] and as single microparticles [31], was investigated by performing a series of *in situ* hydrolysis studies at 70 °C using ATR-FTIR imaging and the multivariate analysis methodology demonstrated in previous work [24].

Fig. 8A–C shows the temporal jet colour MCR-ALS images of un-processed and un-irradiated, 25 kGy γ-irradiated and 100 kGy γ-irradiated PLGA 50/50 particles (upper images) and the corresponding water distribution (lower images) respectively. Although the un-irradiated and 25 kGy irradiated PLGA 50/50 sample images in Fig. 8A and B look similar in the first two time resolved images, a more rapid decrease in the polymer core zone (red) and a larger hydrated layer (from light blue and yellow) can be observed in the 25 kGy irradiated PLGA 50/50 sample images after 5 h, indicating a slightly higher rate of hydrolytic degradation. These differences are more pronounced in the 100 kGy irradiated PLGA 50/50 sample images shown in Fig. 8C, as the polymer core (in red) in the 0 h sample image was observed to disappear after ~2 h indicating a faster rate of polymer degradation. The temporal water distribution images beneath each polymer image in each data set in Fig. 7A–C complement this finding, in that, although the water concentration within the un-irradiated and 25 kGy irradiated microparticles is very low (dark blue) during the first 2 h and then increases gradually (light blue), in the 100 kGy irradiated microparticle, after the first time point, there appears to be no clearly defined core zone where the water intensity would be expected to be low (i.e. dark blue), merely a very large light blue area that becomes lighter in colour indicating higher water content as time proceed, due to the faster hydration presumably because of the irradiated polymer products being more hydrophilic than the un-irradiated one.

As discussed previously, microparticle morphology plays a major role in the hydrolytic degradation of PLGA polymers. SEM analysis of the un-processed and un-irradiated PLGA 50/50, 25 kGy γ-irradiated PLGA 50/50 and 100 kGy γ-irradiated PLGA 50/50 was conducted in order to provide an insight into the effect of gamma irradiation on the microparticle morphology (Fig. 9A–C). The un-irradiated particle has a rough, non-uniform morphology, conversely, the 25 kGy irradiated particle appears to have a much smoother surface. The 100 kGy particle looks quite different to un-irradiated and 25 kGy irradiated microparticles, mainly in that it has a much smoother surface than both and interestingly appears to show some evidence of aggregation of the microparticles.

Applying the NLCF [24] procedure to 5 × 5 pixels binned regions

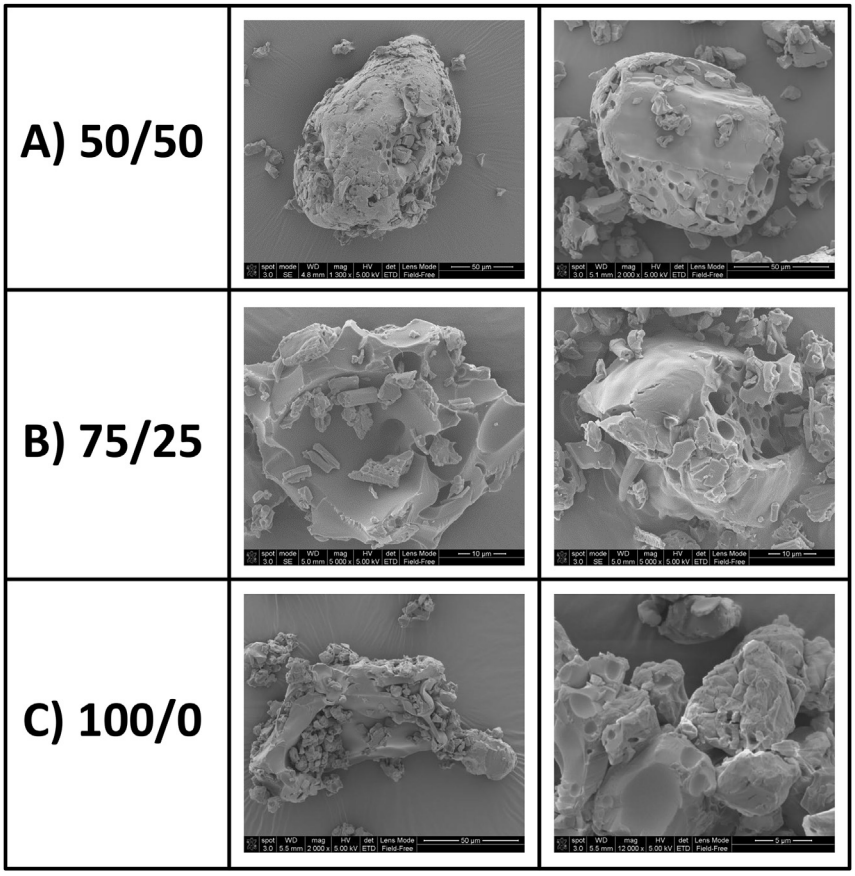

Fig. 6. SEM images of two CriticalMix™ processed PLGA 50/50 (A), PLGA 75/25 (B) and PLA (C) microparticles in each row.

Table 3
Calculated degradation rate constants of the glycolic and lactic units in day^{-1} calculated for different compositions of $scCO_2$ processed PLGAs at 50 °C and 70 °C and un-processed PLGA 50/50 at 70 °C.

L/G	50 °C			70 °C		
	kG	kL	kG/kL	kG	kL	kG/kL
100/0		0.2 ± 0.03			0.4 ± 0.02	
75/25	0.8 ± 0.1	0.6 ± 0.08	1.3	2.1 ± 0.1	1.5 ± 0.1	1.4
50/50	1.1 ± 0.1	0.7 ± 0.11	1.4	2.3 ± 0.2	1.7 ± 0.2	1.4
50/50 un-processed				1.3 ± 0.1	1.0 ± 0.1	1.3

in each image set shown in Fig. 8, hydrolysis rates of both lactic and glycolic units of the un-irradiated, 25 kGy irradiated and 100 kGy irradiated PLGA 50/50 at 70 °C were calculated (Table 4). Gamma irradiation was seen to accelerate the rate of hydrolytic degradation quite dramatically with both glycolic and lactic units having an increased hydrolytic degradation rate as a function of applied gamma dose, the implication being that chain scission is occurring within these microparticles during the irradiation process. Once again the ratio between the degradation rate of glycolic and lactic units was ~1.3, indicating that the relationship between the degradation rates of the two components was independent of gamma dose.

It is well known that when subjected to irradiation, polymers can show a decrease in their molecular weight due to chain scission [42,43]. GPC and DSC are often used to investigate such processes since they facilitate monitoring molecular weight and thermal properties of polymers.

Fig. 10A shows the irradiation dependent change in M_w and PDI of PLGA 50/50 and Fig. 10B shows the change in % M_w with respect to its un-irradiated state to facilitate a better comparison. With increasing γ-irradiation, a decrease in M_w and PDI of the PLGA 50/50 was observed indicating a chain scission mechanism occurring within PLGA 50/50 thus supporting the findings obtained using FTIR imaging.

DSC analyses were conducted on the γ-irradiated and un-irradiated PLGA 50/50 in order to monitor the effect of gamma irradiation on the polymer's thermal properties. Table 5 shows that the T_g of PLGA 50/50 systematically decreases as a function of applied gamma dose. This finding also supported the observation from the GPC data in that PLGA 50/50 was degrading via a chain scission mechanism due to gamma irradiation, with the implication being that the shorter polymer chain lengths require less energy to

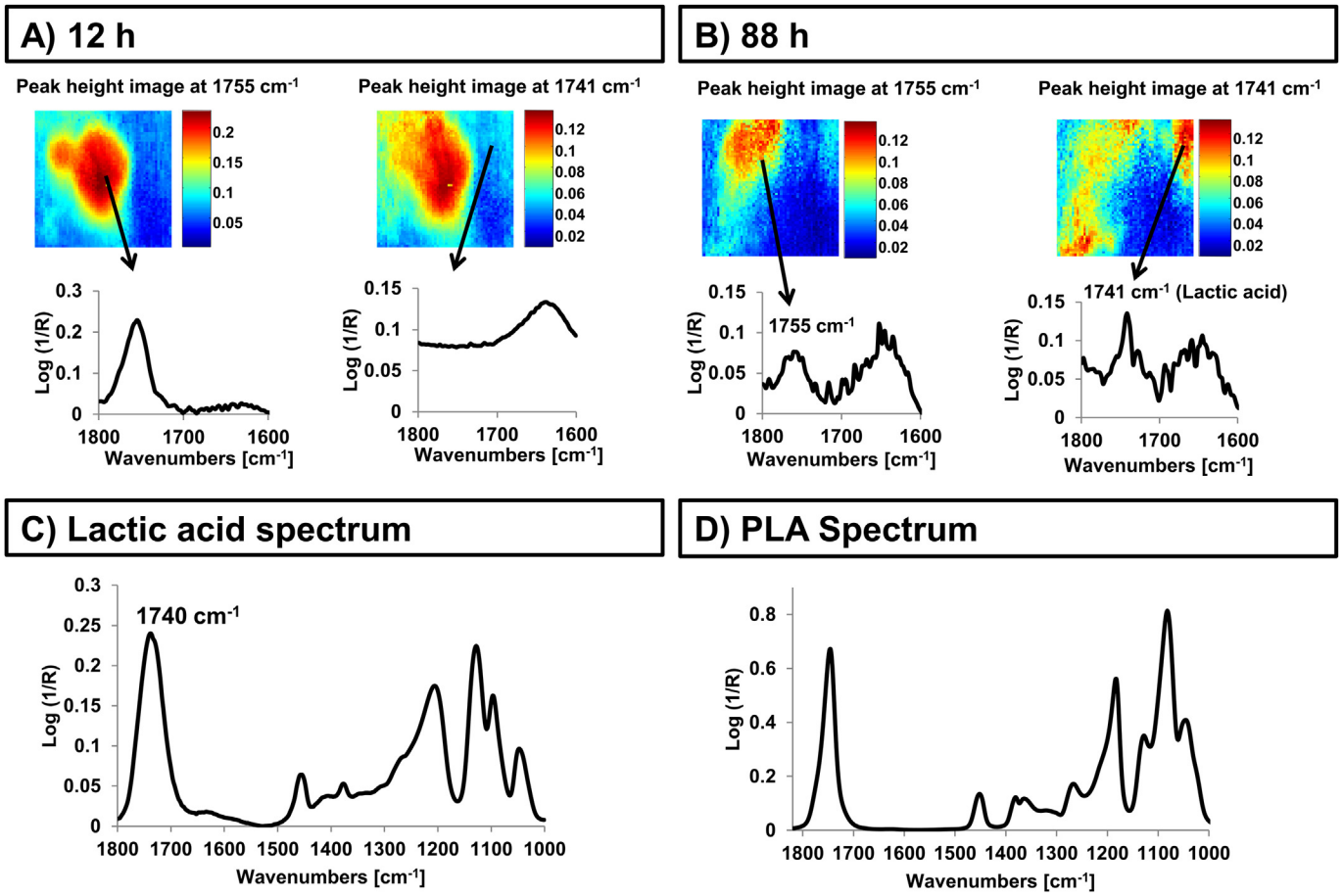

Fig. 7. False colour peak height images of $scCO_2$ processed PLA microparticle undergoing hydrolysis at 70 °C at 1755 cm^{-1} on the left and 1740 cm^{-1} on the right at (A) 12 h and (B) 88 h where pixel spectrum indicated by the arrow is given at the bottom of each of the images. (C) ATR-FTIR spectra of lactic acid and (D) dry PLA. (For interpretation of the references to colour in this figure legend, the reader is referred to the web version of this article.)

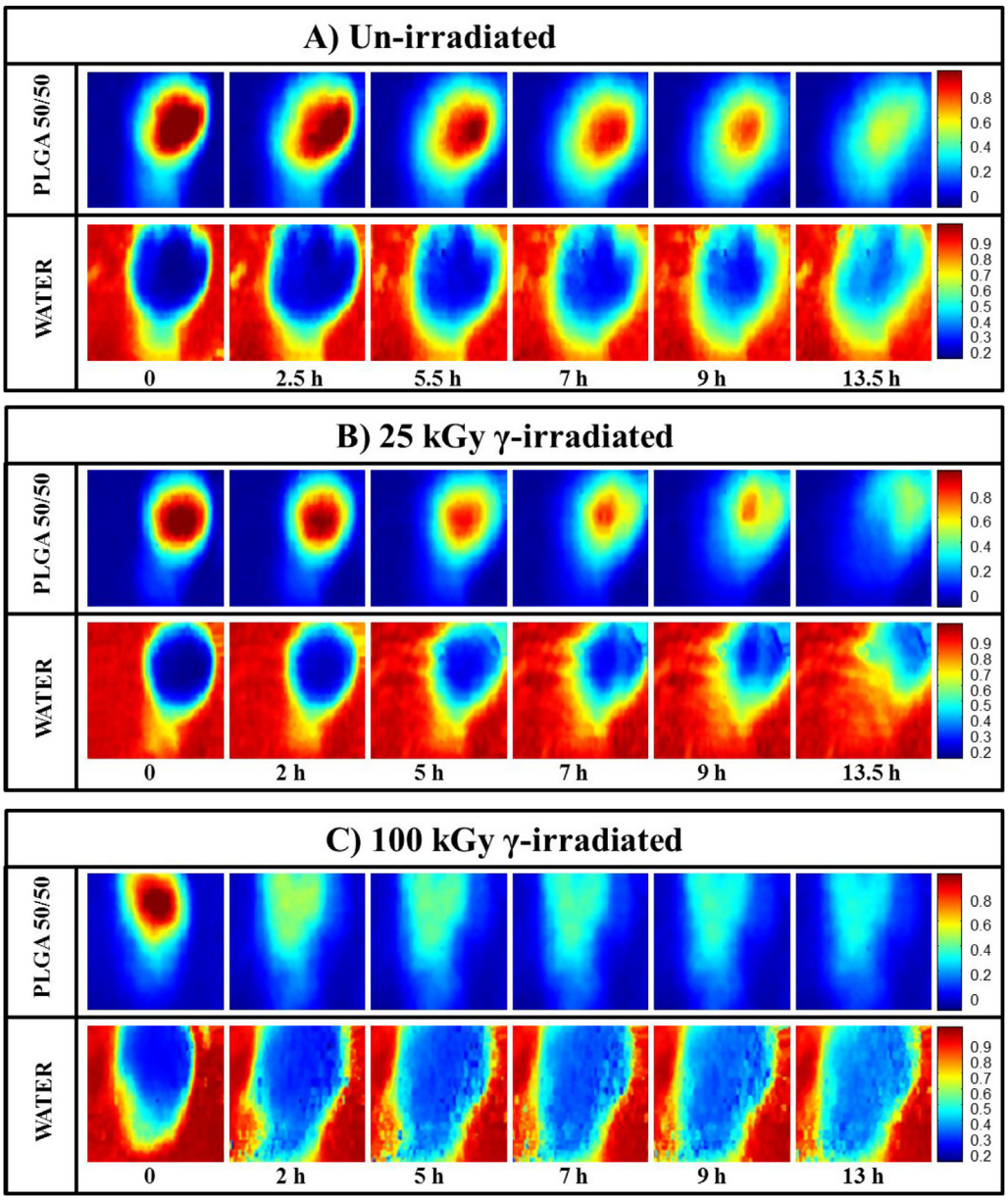

Fig. 8. A set of jet colour IR images representing temporal distribution of PLGA50/50 at 70 °C on the top and water at the bottom for samples that were subject to (A) 0, (B) 25 kGy and (C) 100 kGy γ-irradiation respectively. (For interpretation of the references to colour in this figure legend, the reader is referred to the web version of this article.)

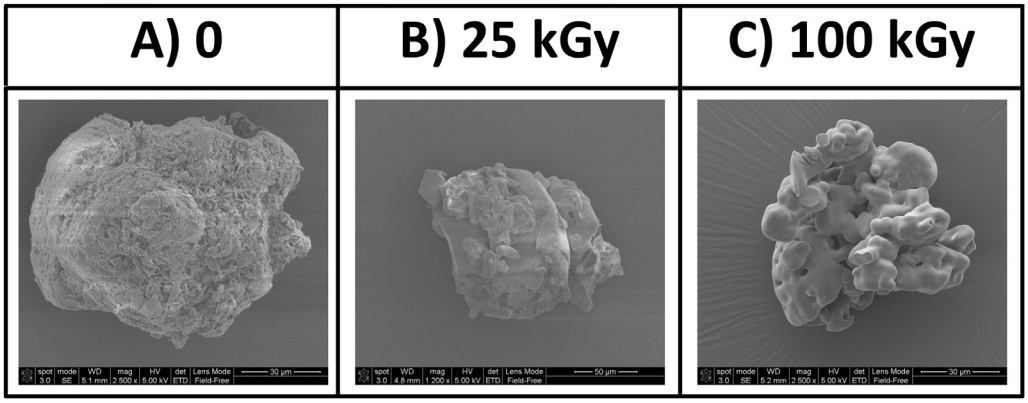

Fig. 9. A set of SEM images un-processed PLGA 50/50 microparticles that are (A) un-irradiated, (B) 25 kGy γ-irradiated and (C) 100 kGy γ-irradiated.

Table 4
Calculated degradation rate constants of the glycolic and lactic units in day^{-1} calculated for un-processed PLGA 50/50 s at 70 °C that were subject to 0, 25 and 100 kGy γ-irradiation.

Gamma dose [kGy]	kL	kG	kG/kL
0	1.0 ± 0.1	1.3 ± 0.1	1.3
25	1.4 ± 0.1	1.8 ± 0.2	1.3
100	1.9 ± 0.3	2.3 ± 0.2	1.2

Table 5
List of glass transition temperatures of un-irradiated and γ-irradiated PLGA50/50.

T_g (°C)	T_g (°C) after 25 kGy γ exposure	T_g (°C) after 100 kGy γ exposure
45.7	43.4	41.9

undergo phase transitions due to an overall reduction in chain entanglement.

All the findings obtained herein via IR imaging, SEM, GPC and DSC were found to be in agreement with those of Nughoro et al. [43] who investigated γ radiation-induced degradation of PLA using GPC and DSC. In their work PLA glass transition temperature (T_g), melting temperature (T_m) and number-average molecular weight (M_n) was shown to decrease with increasing irradiation dose up to 200 kGy, indicating a predominant degradation by random chain-scission. Loo et al. [42] studied e-beam irradiation induced degradation of PLGA films using GPC, DSC and FTIR spectroscopy and also reported a linear relationship between the decrease in molecular weight with respect to radiation dose. In their work, monitoring the reduction in the average molecular weight, T_c, T_g and T_m, it was indicated that the dominant effect of e-beam irradiation on PLGA polymer films was chain scission.

4. Conclusions

Using a combination of FTIR imaging, SEM, DSC and GPC links have been shown between γ-irradiation dose and the rate of hydrolytic degradation based on a range of factors including microparticle morphology and polymer molecular weight. Utilising the chemical discrimination capabilities of FTIR spectroscopy, the degradation rates of glycolic and lactic units in a group of PLGAs were differentiated and quantified.

Using SEM, $scCO_2$ processing was observed to create a porous structure within PLGA microparticles. From the real-time ATR-FTIR imaging hydrolysis study, the findings from the SEM images gave a credible explanation for the higher degradation rate that was observed in the processed microparticles when compared to those which were un-processed.

Degradation rate constants for lactic and glycolic units were shown to decrease with increasing initial lactic content of the copolymer, suggesting that the decreasing ability of a water molecule to diffuse in to an increasingly hydrophobic sample has a high impact on the degradation kinetics of the copolymers within the microparticles. A noticeable decrease in the measured hydrated layer size, determined from the FTIR images, was observed for the $scCO_2$ processed PLGA 50/50 microparticle at 50 °C compared to that of at 70 °C. In addition an increase in temperature resulted in an increase in degradation rates of all PLGAs with different compositions (50/50, 75/25, 100/0) as anticipated. SEM images also indicated that $scCO_2$ processed PLGA 50/50 was more porous than $scCO_2$ processed PLGA 75/25 and this resulted in degradation rate of PLGA 75/25 being less than, but close to that of PLGA 50/50.

The distribution of the degradation product, lactic acid, was probed using FTIR imaging during the hydrolysis of a single PLA microparticle. Lactic acid molecules were observed away from the main region of the PLA microparticle in the aqueous media, indicating that the soluble lactic acid monomers diffused out into the surrounding water resulting in less lactic acid within the core of the PLA microparticle. It is believe that this is the first time such evidence has been observed within a degrading PLA microparticle in its natural environment without modifying the sample using any chemical markers or dyes.

The effect of γ-irradiation on the hydrolytic degradation behaviour of PLGA 50/50 polymer microparticles was also investigated. SEM images indicated a decrease in surface roughness as a function of increased applied gamma dose for all formulations. The 100 kGy irradiated PLGA 50/50 microparticles were found to show evidence of aggregation and looked smoother compared to those un-irradiated and 25 kGy irradiated. FTIR imaging also indicated a noticeable increase in water uptake in the 100 kGy γ-irradiated PLGA 50/50 microparticle compared to the others and this was thought to be a result of the severe change in morphology of the former as shown in the SEM images. IR imaging data revealed that the measured degradation rate increased as a function of increasing gamma dose. This observation was supported by GPC analysis; indicating a decrease in molecular weight of the PLGA 50/50 samples with increased gamma irradiation and DSC analysis; samples exhibited a decrease in the T_g of PLGA 50/50 as a function of applied gamma dose. All these findings indicate a chain scission degradation mechanism upon gamma irradiation.

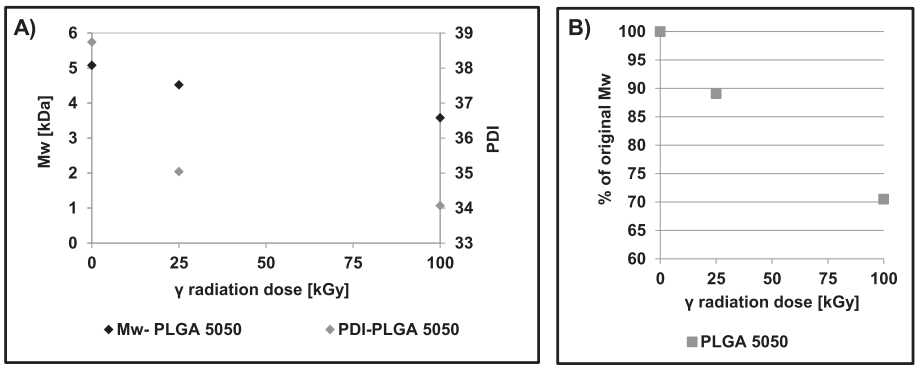

Fig. 10. GPC results for non-irradiated and irradiated PLGA 50/50 showing the changes in M_w and PDI in (A) and % change in polymer's M_w with respect to its un-irradiated state, to facilitate better comparison in (B).

Acknowledgements

This research was supported by a grant from Engineering and Physical Sciences Research Council (EPSRC) grant number EP/I501665/1. The underlying research data can be accessed via http://doi.org/10.17032/shu-150002 and are available to view/consult/re-use on a standard ODC-By licence.

References

[1] C.F. van der Walle, O. Olejnik, Chapter 1 – an overview of the field of peptide and protein delivery, in: C.F. van der Walle (Ed.), Peptide and protein delivery, Academic Press, Boston, 2011, pp. 1–22.
[2] K.E. Uhrich, S.M. Cannizzaro, R.S. Langer, K.M. Shakesheff, Polymeric systems for controlled drug release, Chem Rev 99 (1999) 3181–3198.
[3] R. Langer, Controlled release of a therapeutic protein, Nat Med 2 (1996) 742–743.
[4] O. Hiroaki, Y. Masaki, H. Toshiro, I. Yayoi, K. Shigeru, O. Yasuaki, et al., Drug delivery using biodegradable microspheres, J Control Release 28 (1994) 121–129.
[5] S.S. Davis, L. Illum, S. Stolnik, Polymers in drug delivery, Curr Opin Colloid Interface Sci 1 (1996) 660–666.
[6] C. Wischke, S.P. Schwendeman, Principles of encapsulating hydrophobic drugs in PLA/PLGA microparticles, Int J Pharm 364 (2008) 298–327.
[7] U. Edlund, A.C. Albertsson, Degradable aliphatic polyesters, Adv Polym Sci 157 (2002) 67–112.
[8] D. Lemoine, C. Francois, F. Kedzierewicz, V. Preat, M. Hoffman, P. Maincent, Stability study of nanoparticles of poly(ε-caprolactone), poly(d,l-lactide) and poly(d,l-lactide-co-glycolide), Biomaterials 17 (1996) 2191–2197.
[9] S. Schwendeman, Recent advances in the stabilization of proteins encapsulated in injectable PLGA delivery systems, Crit Rev Ther Drug Carr Syst 19 (2002) 73–98.
[10] D. Blanco, M.J. Alonso, Protein encapsulation and release from poly(lactide-co-glycolide) microspheres: effect of the protein and polymer properties and of the co-encapsulation of surfactants, Eur J Pharm Biopharm 45 (1998) 285–294.
[11] W.B. Liechty, D.R. Kryscio, B.V. Slaughter, N.A. Peppas, Polymers for drug delivery systems, Annu Rev Chem Biomol Eng 1 (2010) 149–173.
[12] C.E. Upton, C.A. Kelly, K.M. Shakesheff, S.M. Howdle, One dose or two? the use of polymers in drug delivery, Polym Int 56 (2007) 1457–1460.
[13] R.C. Mundargi, V.R. Babu, V. Rangaswamy, P. Patel, T.M. Aminabhavi, Nano/micro technologies for delivering macromolecular therapeutics using poly(d,l-lactide-co-glycolide) and its derivatives, J Control Release 125 (2008) 193–209.
[14] P.A. Rivera, M. Martinez-Oharriz, M. Rubio, J.M. Irache, S. Espuelas, Fluconazole encapsulation in PLGA microspheres by spray-drying, J Microencapsul 21 (2004) 203–211.
[15] C.A. Kelly, S.M. Howdle, A. Naylor, G. Coxhill, L.C. Tye, L. Illum, et al., Stability of human growth hormone in supercritical carbon dioxide, J Pharm Sci 101 (2012) 56–67.
[16] M.L. Houchin, E.M. Topp, Chemical degradation of peptides and proteins in PLGA: a review of reactions and mechanisms, J Pharm Sci 97 (2008) 2395–2404.
[17] R.A. Kenley, M.O. Lee, T.R. Mahoney, L.M. Sanders, Poly(lactide-co-glycolide) decomposition kinetics in vivo and in vitro, Macromolecules 20 (1987) 2398–2403.
[18] T.G. Park, Degradation of poly(lactic-co-glycolic acid) microspheres: effect of copolymer composition, Biomaterials 16 (1995) 1123–1130.
[19] M.A. Tracy, K.L. Ward, L. Firouzabadian, Y. Wang, N. Dong, R. Qian, et al., Factors affecting the degradation rate of poly(lactide-co-glycolide) microspheres in vivo and in vitro, Biomaterials 20 (1999) 1057–1062.
[20] K. Odelius, A. Hoglund, S. Kumar, M. Hakkarainen, A.K. Ghosh, N. Bhatnagar, et al., Porosity and pore size regulate the degradation product profile of polylactide, Biomacromolecules 12 (2011) 1250–1258.
[21] E. Vey, C. Rodger, J. Booth, M. Claybourn, A.F. Miller, A. Saiani, Degradation kinetics of poly(lactic-co-glycolic) acid block copolymer cast films in phosphate buffer solution as revealed by infrared and Raman spectroscopies, Polym Degrad Stab 96 (2011) 1882–1889.
[22] C.M. Agrawal, D. Huang, J.P. Schmitz, K.A. Athanasiou, Elevated temperature degradation of a 50:50 copolymer of PLA-PGA, Tissue Eng 3 (1997) 345–352.
[23] F. Alexis, S. Venkatraman, S.K. Rath, L.H. Gan, Some insight into hydrolytic scission mechanisms in bioerodible polyesters, J Appl Polym Sci 102 (2006) 3111–3117.
[24] H. Keles, A. Naylor, F. Clegg, C. Sammon, The application of non-linear curve fitting routines to the analysis of mid-infrared images obtained from single polymeric microparticles, Analyst 139 (2014) 2355–2369.
[25] P.A. Burke, Determination of internal pH in PLGA microspheres using 31P NMR spectroscopy, Proc Int Symp Control Release Bioact Mater 23 (1996) 133–134.
[26] A. Brunner, K. Mäder, A. Göpferich, pH and osmotic pressure inside biodegradable microspheres during erosion, Pharm Res 16 (1999) 847–853.
[27] A.G. Ding, S.P. Schwendeman, Acidic microclimate pH distribution in PLGA microspheres monitored by confocal laser scanning microscopy, Pharm Res 25 (2008) 2041–2052.
[28] K. Fu, D. Pack, A. Klibanov, R. Langer, Visual evidence of acidic environment within degrading poly(lactic-co-glycolic acid) (PLGA) microspheres, Pharm Res 17 (2000) 100–106.
[29] L. Li, S.P. Schwendeman, Mapping neutral microclimate pH in PLGA microspheres, J Control Release 101 (2005) 163–173.
[30] F. Jordan, A. Naylor, C.A. Kelly, S.M. Howdle, A. Lewis, L. Illum, Sustained release hGH microsphere formulation produced by a novel supercritical fluid technology: in vivo studies, J Control Release 141 (2010) 153–160.
[31] H. Keles, A. Naylor, F. Clegg, C. Sammon, Studying the release of hGH from gamma-irradiated PLGA microparticles using ATR-FTIR imaging, Vib Spectrosc 71 (2014) 76–84.
[32] M.J. Whitaker, J. Hao, O.R. Davies, G. Serhatkulu, S. Stolnik-Trenkic, S.M. Howdle, et al., The production of protein-loaded microparticles by supercritical fluid enhanced mixing and spraying, J Control Release 101 (2005) 85–92.
[33] J. Hao, M.J. Whitaker, B. Wong, G. Serhatkulu, K.M. Shakesheff, S.M. Howdle, Plasticization and spraying of poly (DL-lactic acid) using supercritical carbon dioxide: control of particle size, J Pharm Sci 93 (2004) 1083–1090.
[34] J. Hao, M.J. Whitaker, G. Serhatkulu, K.M. Shakesheff, S.M. Howdle, Supercritical fluid assisted melting of poly(ethylene glycol): a new solvent-free route to microparticles, J Mater Chem 15 (2005) 1148–1153.
[35] V. Klang, C. Valenta, N.B. Matsko, Electron microscopy of pharmaceutical systems, Micron 44 (2013) 45–74.
[36] T.G. Park, W. Lu, G. Crotts, Importance of in vitro experimental conditions on protein release kinetics, stability and polymer degradation in protein encapsulated poly (d,l-lactic acid-co-glycolic acid) microspheres, J Control Release 33 (1995) 211–222.
[37] M. Vert, S.M. Li, H. Garreau, Attempts to map the structure and degradation characteristics of aliphatic polyesters derived from lactic and glycolic acids, J Biomater Sci Polym 6 (1994) 639–649.
[38] E. Vey, C. Roger, L. Meehan, J. Booth, M. Claybourn, A.F. Miller, et al., Degradation mechanism of poly(lactic-co-glycolic) acid block copolymer cast films in phosphate buffer solution, Polym Degrad Stab 93 (2008) 1869–1876.
[39] L. Chen, R.N. Apte, S. Cohen, Characterization of PLGA microspheres for the controlled delivery of IL-1α for tumor immunotherapy, J Control Release 43 (1997) 261–272.
[40] D.K.- Xing, D.T. Crane, B. Bolgiano, M.J. Corbel, C. Jones, D. Sesardic, Physicochemical and immunological studies on the stability of free and microsphere-encapsulated tetanus toxoid in vitro, Vaccine 14 (1996) 1205–1213.
[41] M.B. Sintzel, A. Merkli, C. Tabatabay, R. Gurny, Influence of irradiation sterilization on polymers used as drug Carriers—A review, Drug Dev Ind Pharm 23 (1997) 857–878.
[42] J.S.C. Loo, C.P. Ooi, F.Y.C. Boey, Degradation of poly(lactide-co-glycolide) (PLGA) and poly(l-lactide) (PLLA) by electron beam radiation, Biomaterials 26 (2005) 1359–1367.
[43] P. Nugroho, H. Mitomo, F. Yoshii, T. Kume, Degradation of poly(l-lactic acid) by γ-irradiation, Polym Degrad Stab 72 (2001) 337–343.